Neoadjuvant and Adjuvant Pembrolizumab in Resectable Locally Advanced, Human Papillomavirus–Unrelated Head and Neck Cancer: A Multicenter, Phase II Trial

Ravindra Uppaluri[1,2], Katie M. Campbell[3,4], Ann Marie Egloff[1], Paul Zolkind[5], Zachary L. Skidmore[4], Brian Nussenbaum[5,6], Randal C. Paniello[5,6], Jason T. Rich[5,6], Ryan Jackson[5,6], Patrik Pipkorn[5,6], Loren S. Michel[6,7], Jessica Ley[7], Peter Oppelt[6,7], Gavin P. Dunn[6,8], Erica K. Barnell[3,4], Nicholas C. Spies[4], Tianxiang Lin[5], Tiantian Li[9], David T. Mulder[9], Youstina Hanna[9], Iulia Cirlan[9], Trevor J. Pugh[9,10,11], Tenny Mudianto[2], Rachel Riley[2], Liye Zhou[2], Vickie Y. Jo[1], Matthew D. Stachler[12], Glenn J. Hanna[2], Jason Kass[1,2], Robert Haddad[1,2], Jonathan D. Schoenfeld[2,13], Evisa Gjini[12], Ana Lako[12], Wade Thorstad[6,14], Hiram A. Gay[6,14], Mackenzie Daly[6,14], Scott J. Rodig[12,15], Ian S. Hagemann[16], Dorina Kallogjeri[5], Jay F. Piccirillo[5,6], Rebecca D. Chernock[16], Malachi Griffith[3,4,6,7], Obi L. Griffith[3,4,6,7], and Douglas R. Adkins[6,7]

ABSTRACT

Purpose: Pembrolizumab improved survival in patients with recurrent or metastatic head and neck squamous-cell carcinoma (HNSCC). The aims of this study were to determine if pembrolizumab would be safe, result in pathologic tumor response (pTR), and lower the relapse rate in patients with resectable human papillomavirus (HPV)–unrelated HNSCC.

Patients and Methods: Neoadjuvant pembrolizumab (200 mg) was administered and followed 2 to 3 weeks later by surgical tumor ablation. Postoperative (chemo)radiation was planned. Patients with high-risk pathology (positive margins and/or extranodal extension) received adjuvant pembrolizumab. pTR was quantified as the proportion of the resection bed with tumor necrosis, keratinous debris, and giant cells/histiocytes: pTR-0 (<10%), pTR-1 (10%–49%), and pTR-2 (≥50%). Coprimary endpoints were pTR-2 among all patients and 1-year relapse rate in patients with high-risk pathology (historical: 35%). Correlations of baseline PD-L1 and T-cell infiltration with pTR were assessed. Tumor clonal dynamics were evaluated (ClinicalTrials.gov NCT02296684).

Results: Thirty-six patients enrolled. After neoadjuvant pembrolizumab, serious (grades 3–4) adverse events and unexpected surgical delays/complications did not occur. pTR-2 occurred in eight patients (22%), and pTR-1 in eight other patients (22%). One-year relapse rate among 18 patients with high-risk pathology was 16.7% (95% confidence interval, 3.6%–41.4%). pTR ≥10% correlated with baseline tumor PD-L1, immune infiltrate, and IFNγ activity. Matched samples showed upregulation of inhibitory checkpoints in patients with pTR-0 and confirmed clonal loss in some patients.

Conclusions: Among patients with locally advanced, HPV-unrelated HNSCC, pembrolizumab was safe, and any pathologic response was observed in 44% of patients with 0% pathologic complete responses. The 1-year relapse rate in patients with high-risk pathology was lower than historical.

Introduction

Patients with head and neck squamous-cell carcinoma (HNSCC) usually present with locally advanced disease. Surgery or definitive (chemo)radiation is the initial treatment in many of these patients. A large subset of surgically treated patients have high-risk pathology features (positive margin and/or extranodal extension) that are best treated with intensive postoperative adjuvant cisplatin and radiation therapy (POACRT). However, 35% of patients, particularly those with human papillomavirus (HPV)–unrelated HNSCC, will develop

[1]Department of Surgery, Brigham and Women's Hospital, Boston, Massachusetts. [2]Department of Medical Oncology, Dana-Farber Cancer Institute, Boston, Massachusetts. [3]Department of Genetics, Washington University School of Medicine, St. Louis, Missouri. [4]McDonnell Genome Institute, Washington University School of Medicine, St. Louis, Missouri. [5]Department of Otolaryngology, Washington University School of Medicine, St. Louis, Missouri. [6]Alvin J. Siteman Cancer Center, Washington University School of Medicine, St. Louis, Missouri. [7]Department of Medicine/Medical Oncology, Washington University School of Medicine, St. Louis, Missouri. [8]Department of Neurological Surgery, Washington University School of Medicine, St. Louis, Missouri. [9]Princess Margaret Cancer Center, University Health Network, Toronto, Ontario, Canada. [10]Department of Medical Biophysics, University of Toronto, Toronto, Ontario, Canada. [11]Ontario Institute for Cancer Research, Toronto, Ontario, Canada. [12]Department of Pathology, Brigham and Women's Hospital, Boston, Massachusetts. [13]Department of Radiation-Oncology, Brigham and Women's Hospital, Boston, Massachusetts. [14]Department of Radiation-Oncology, Washington University School of Medicine, St. Louis, Massachusetts. [15]Center for Immuno-Oncology, Brigham and Women's Hospital, Boston, Massachusetts. [16]Department of Pathology and Immunology, Washington University School of Medicine, St. Louis, Missouri.

Note: Supplementary data for this article are available at Clinical Cancer Research Online (http://clincancerres.aacrjournals.org/).

Corrected online November 25, 2020.

R. Uppaluri and K.M. Campbell contributed equally to this article.

R. Uppaluri, O.L. Griffith, and D.R. Adkins contributed equally as the co-senior authors of this article.

Current address for K.M. Campbell: Division of Hematology-Oncology, Department of Medicine, University of California, Los Angeles, Los Angeles, California.

Corresponding Author: Ravindra Uppaluri, Dana-Farber/Brigham and Women's Cancer Center, 450 Brookline Avenue, Boston, MA 02215. Phone: 617-632-3091; Fax: 617-632-5786; E-mail: Ravindra_Uppaluri@DFCI.Harvard.edu

Clin Cancer Res 2020;26:5140–52

doi: 10.1158/1078-0432.CCR-20-1695

Translational Relevance

Many patients with locally advanced, human papillomavirus–unrelated head and neck squamous-cell carcinoma (HNSCC) undergo multimodality therapy, including surgery followed by adjuvant (chemo)radiation therapy. Outcomes are suboptimal, especially for high-risk patients (positive margins and/or extranodal extension). Novel treatment intensification approaches are needed. As blocking mAbs to the programmed death-1 pathway have improved patient outcomes across several cancer types, their integration into definitive surgical management is a logical next step. In this study, we completed a phase II clinical trial with neoadjuvant and adjuvant pembrolizumab in patients with HNSCC undergoing standard-of-care surgical therapy. We found this approach was safe in the surgical setting, identified pathologic changes induced by neoadjuvant pembrolizumab, and defined pathologic and genomic biomarkers of response and potential for clinical impact. Together, these findings highlight pembrolizumab integration into the definitive surgical management of locally advanced HNSCC as a rational approach that warrants testing in the phase III setting.

relapse of disease (1, 2). Attempts to improve this outcome have been unsuccessful (3). Novel treatment strategies are needed for these patients.

Immune checkpoint inhibitors could reduce the risk of disease relapse in resectable locally advanced, HPV-negative HNSCC. Randomized trials showed that pembrolizumab and nivolumab, inhibitors of the programmed death receptor-1 (PD-1), improved overall survival (OS) of patients with platinum-resistant HNSCC (4, 5). Pembrolizumab given alone or with chemotherapy improved the OS of patients with untreated recurrent or metastatic disease (6). The results of these trials provide strong rationale for evaluating the clinical impact of immune checkpoint inhibitors in patients with resectable locally advanced, HPV-unrelated HNSCC.

Immunotherapy may be administered before (neoadjuvant) or after (adjuvant) surgery. Preclinical experiments with several cancer types showed that administration of immunotherapy in the neoadjuvant interval provided greater benefit than when given in the adjuvant interval (7–9). In mouse models of spontaneously metastatic breast cancer, neoadjuvant immunotherapy and surgery were more effective in generating tumor-specific $CD8^+$ T cells and preventing development of lethal metastases than surgery alone (7, 8). Importantly, the benefit of immunotherapy was dependent on resection of the primary tumor. In syngeneic mouse models of HPV-unrelated oral cavity carcinoma with defined T-cell antigens, administration of PD-1 inhibitor before, but not after, surgery reversed functional immunodominance and induced effector T-cell immunity that resulted in rejection of tumor rechallenge after surgery (9). Collectively, these data support the critical importance of coordinating administration of immunotherapy before surgery to achieve optimal disease control with this novel strategy.

In addition to improved disease control, administration of immune checkpoint inhibitors in the neoadjuvant interval could result in other clinical benefits, including reduction of the rate of high-risk pathology and downstaging of the cancer. These outcomes could alter the selection of adjuvant therapy, resulting in less intense treatment. Finally, matched tumor tissue obtained at baseline and at surgery can be evaluated to define biomarkers that predict tumor response and resistance to immune checkpoint inhibitors. HNSCC is ideally suited for testing the effect of administration of immune checkpoint inhibitors in the neoadjuvant interval. Tumor is readily accessible to obtain matched baseline and surgical tissue and to perform visual assessments of tumor response (10). Although reported in a few other cancers (11–20), the safety and biologic and clinical effects of administration of immune checkpoint inhibitors have not been reported in a patient cohort with resectable locally advanced HPV-unrelated HNSCC.

In this multicenter, phase II trial, we aimed to determine if administration of neoadjuvant pembrolizumab to patients with resectable locally advanced, HPV-unrelated HNSCC would be safe and result in pathologic tumor responses (pTR). We evaluated the immunologic correlates to pTR and assessed tumor clonal dynamics in matched tumor samples obtained before and after neoadjuvant pembrolizumab. Among patients with high-risk pathology, we aimed to determine if administration of neoadjuvant and adjuvant pembrolizumab would result in a relapse rate lower than historical. Herein, we report the results of our trial.

Patients and Methods

Study design and participants

We did a multicenter, phase II trial at two university sites in the United States: Washington University, St. Louis, MO, and Dana-Farber/Brigham and Women's Cancer Center, Boston, MA. The protocol is included in the Supplementary Materials. The trial is a nonrandomized two-group study. Patient selection criteria were the same for both groups. Group 1 completed enrollment before group 2 accrued patients. Group 1 is reported here. In group 1, patients were treated with one dose of neoadjuvant pembrolizumab, followed by surgery. Patients with high-risk pathology were scheduled to be treated with POACRT followed by adjuvant pembrolizumab; patients without high-risk pathology were scheduled to be treated with POART or observation but not adjuvant pembrolizumab. In group 2, patients were treated with two doses of neoadjuvant pembrolizumab, followed by surgery, then POACRT if high-risk pathology or POART (or observation) if without high-risk pathology. Group 2 did not receive adjuvant pembrolizumab. Group 2 is ongoing, having accrued 25 of the planned sample size of 31 patients; the data are not yet mature. The results of group 2 will be reported at a later date.

Eligible patients had resectable clinical stage III–IVb (AJCC, 7th Edition), HPV-unrelated (oral cavity, larynx, hypopharynx or p16-negative oropharynx) HNSCC, measurable disease per RECIST v1.1, Eastern Cooperative Oncology Group performance status 0–1, and adequate marrow and organ function [absolute neutrophil count ≥1,500/mcL, platelets ≥100,000/mcL, hemoglobin ≥9g/dL; total bilirubin ≤1.5x upper limits of normal (ULN), AST and ALT ≤2.5x ULN; serum creatinine ≤1.5x ULN or creatinine clearance ≥30 mL/min]. Key exclusion criteria included HPV-related oropharynx SCC, active autoimmune disease, or immunodeficiency.

Tests required to determine eligibility included complete blood count, metabolic panel, pregnancy test (women), coagulation and thyroid panels, urinalysis, and CT scans of the neck and chest.

Procedures

In group 1, patients received one dose of pembrolizumab (200 mg, IV) 13 to 22 days before (neoadjuvant) surgery. Surgery included resection of all gross disease at the primary site, ipsilateral (and contralateral, in some patients) therapeutic/prophylactic neck dissection, and reconstruction using pedicled or free-flap procedures as

deemed appropriate. Surgical plan and extent of surgical tumor resection was defined by baseline assessments obtained before neoadjuvant pembrolizumab and did not change if treatment responses were observed. Patients with high-risk pathology were scheduled to be treated with POACRT, if they had adequate organ function and had recovered from surgery (1, 2). Upon resolution of POACRT-related adverse events (AEs) to ≤grade one and after 3 months from surgery date, patients with high-risk pathology were scheduled to be treated with adjuvant pembrolizumab (200 mg) every 3 weeks for six doses. Dose delays of pembrolizumab and treatment of immune-related AEs were performed per protocol. Patients without high-risk pathology (low/intermediate-risk) were scheduled to be treated with POART (or observation), but not adjuvant pembrolizumab. Physician discretion in selection of standard-of-care adjuvant therapy was permitted in patients with intermediate-risk pathology, such that some patients were treated with POACRT even though they lacked traditional high-risk-pathology. Administration of POA(C)RT was performed per protocol.

Before neoadjuvant pembrolizumab, patients underwent baseline assessment by physical examination and CT scan of the neck, and a biopsy of the primary tumor and collection of peripheral blood for correlative studies. Patients were assessed by physical examination the day before or day of surgery. After patient 20, the trial was amended to perform a CT scan of the neck within 10 days prior to surgery. On the day of surgery, tissue from the primary tumor and peripheral blood were collected for correlative studies. AEs were assessed using revised Common Terminology Criteria for Adverse Events v4.0. Perisurgical AEs were assessed using Clavien–Dindo Classification of Surgical Complications (21). Tumor response was assessed using RECISTv1.1. Patients were monitored for 30 days after surgery for AEs and surgical/wound-healing complications. During the administration of adjuvant pembrolizumab, patients were assessed every 3 weeks beginning with the first dose of pembrolizumab by physical examination, complete blood count, and metabolic panel, and every 6 weeks by thyroid panel and urinalysis. In these patients, AEs were monitored for 90 days after the last dose of adjuvant pembrolizumab. Patients were monitored for relapse every 3 months after surgery by physical examination and CT scans.

Details of PD-L1 IHC and multiplex immunofluorescence (MIF) are described in the Supplementary Appendix. Details regarding whole-exome sequencing (WES), performed on tumor samples and matched normal blood, RNA sequencing (RNA-seq) on tumor samples, T-cell receptor sequencing (CapTCR-seq; ref. 22) on peripheral blood, multisector targeted genome sequencing on tumor samples, and analyses (expression, deconvolution, TCR repertoire, etc.) are provided in the Supplementary Appendix. DNA and RNA data were processed using the Genome Modeling System (23, 24). Sequencing data have been deposited in dbGaP (phs001623). Patient HLA haplotypes and mutational profiles were used to predict putative neoantigens with pVACtools (25).

Outcomes

The coprimary endpoints were 1-year relapse rate (the absolute proportion of patients who developed local–regional and/or distant relapse within 1 year of surgery) in patients with high-risk pathology, and the proportion of all patients with pTR-2 in the surgical specimen after administration of one dose of neoadjuvant pembrolizumab. pTR was defined as the presence of tumor cell necrosis and keratinous debris with giant cell/histiocytic reaction, quantified as a percentage of the overall tumor bed (area pathologic response/area pathologic response plus viable tumor): pTR-0 (<10%), pTR-1 (10%–49%), and pTR-2 (≥50%). Two pathologists with head and neck expertise (R.D. Chernock and I.S. Hagemann) independently evaluated all slides from baseline and surgery specimens and quantified pTR in increments of 10%. Primary tumor and lymph node metastases were scored separately. Overall pTR was classified based on the best pTR observed in either primary tumor or lymph node. Joint review consensus was reached when discrepancies occurred. Current standardized definitions of immune checkpoint inhibitor–induced pTR were not available when the study was begun, and were not used in the analysis. Secondary endpoints included safety of administration of neoadjuvant pembrolizumab and clinical tumor response to neoadjuvant pembrolizumab assessed by physical examination and, in some patients, by RECISTv1.1. Correlative endpoints assessed on matched tumor specimens obtained before and after (on day of surgery) neoadjuvant pembrolizumab included PD-L1 expression, histologic, immunologic, genomic, and tumor clonal dynamic changes. T-cell clonality was performed on peripheral blood obtained before and after neoadjuvant pembrolizumab (Supplementary Table S1).

No major protocol deviations occurred. The protocol was amended six times over the course of the study. Amendments 1 to 3 included updates of the risk profile and dose modifications of study drug, clarified eligibility criteria, and added Dana-Farber/Brigham and Women's Cancer Center, Boston, MA, as a secondary site. Amendment 4 added correlative studies. Amendment 5 added an unplanned interim analysis after the first 20 patients enrolled into group 1 due to the lower-than-expected rate of patients with high-risk pathology, and added CT scan of the neck to be performed after neoadjuvant pembrolizumab and prior to surgery. Amendment 6 closed accrual to group 1, and added group 2.

Statistical analysis

Relapse rate at 1 year in patients with high-risk pathology was the initial primary endpoint. Historic data showed that the 1-year relapse rate after surgery and POACRT in patients with high-risk pathology was 35% (1, 2). Relapse rate at 1 year was selected because the majority (>90%) of relapse events in these patients occurred within 1 year of surgery (1, 2). A sample size of 31 evaluable patients was required to detect a reduction in the 1-year relapse rate to ≤20%, with a power of 80%, using a one-sided alpha of 0.05. Evaluable patients for this endpoint were those who had high-risk pathology in the surgical specimen after one dose of neoadjuvant pembrolizumab. Assuming a rate of high-risk pathology of 80% in patients with clinical stage III/IV HPV-unrelated HNSCC, and a 20% drop-out rate, we planned to accrue a total of 46 patients to group 1. However, after enrollment of the first 20 patients, the proportion of patients with high-risk pathology after one dose of neoadjuvant pembrolizumab and surgery was lower than expected (35%), prompting an unplanned interim analysis to assess the feasibility to achieve the initial primary endpoint. Enrollment continued during the interim analysis. The results of the interim analysis confirmed the unexpectedly lower rate of high-risk pathology. The trial was amended to (i) close enrollment of group 1 based on inability to accrue the required number of patients with high-risk pathology in a practical interval, (ii) addition of pTR-2 after neoadjuvant pembrolizumab in all patients as a coprimary endpoint, and (iii) addition of group 2, as previously described. In this report, the analysis of 1-year relapse rate in patients with high-risk pathology was performed as intention to treat.

Stopping rules were in place for delay of surgery or serious (grade 3–5) AEs attributed to pembrolizumab. The study was to be stopped, and amended or closed, in the event of (i) neoadjuvant pembrolizumab-related AEs leading to significant delay in surgery (more than

14 days delay in one of the first 15 patients, two of 30, or three of 45) or (ii) serious pembrolizumab-related AEs (occurring in one of the first 10 patients, two of 20, three of 30, four of 40, or five of all patients).

Distribution of demographic and clinical characteristics was defined and compared between patients in high-risk and other (low/intermediate-risk) pathology groups. Percent difference and 95% confidence intervals (CIs) were calculated for categorical variables; median difference and 95% CI were calculated for continuous variables. Spearman's rank correlation coefficient was used to estimate correlations between tumor PD-L1 staining and numbers of tumor-infiltrating T cells ($CD8^+$ and $CD4^+$) and extent of pTR. Molecular correlates were evaluated for changes across pTR categories using the nonparametric test of trend. Kaplan–Meier estimates of OS, progression-free survival (PFS), and relapse-free survival (RFS) rates and 95% CI by pathology risk category or pTR category were determined and differences between categories assessed using the log rank test. OS was defined as time (months) from day of surgery to death; PFS was defined as time from day of surgery to first disease progression event (new primary, recurrence, distant metastasis, or death from disease) or death from any cause; RFS was defined as time from day of surgery to first relapse event (recurrence or distant metastasis). In gene expression analysis, unpaired Mann–Whitney/Wilcoxon rank-sum tests were used to compare the immune cell populations across groups of patients, and paired Wilcoxon signed-rank tests were used to compare matched baseline and posttreatment tumor samples. Differential gene expression analysis was performed using the Wald test across groups.

Study approval

The study protocol was approved by the Institutional Review Board at each participating site and registered nationally (ClinicalTrials.gov NCT02296684). All patients provided written, signed, informed consent to participate. This study followed ethical guidelines of the Declaration of Helsinki, Belmont Report, and the U.S. Common Rule. Independent data monitoring was done by the quality assurance committee of Washington University (St. Louis, MO).

Role of the funding source

The funders had no role in the study design, data collection, data analysis, data interpretation, or writing of the report. All authors had full access to all data in the study. The corresponding author had final responsibility for the decision to submit for publication.

Results

Between June 30, 2015, and March 30, 2018, 36 patients enrolled into group 1 of the trial. Patient and tumor characteristics were typical of those observed in patients with locally advanced, HPV-unrelated HNSCC: mostly males with a smoking history and large tumors (**Table 1**). The trial profile is shown in **Fig. 1A**. All patients received one dose of neoadjuvant pembrolizumab and underwent surgery. Microvascular flap reconstruction was required in 28 patients. Eighteen patients (50%) had high-risk pathology, of which 12 were treated with POACRT and adjuvant pembrolizumab, four with POACRT, one with POART, and one was observed (Supplementary Table S2). Adjuvant pembrolizumab was not administered to six patients with high-risk pathology due to persistent toxicity of POACRT (2), patient decision (2), perioperative myocardial infarction (1), and interim development of distant metastasis (1). Eighteen patients (50%) had low/intermediate-risk pathology, of which 10 were treated with POART, four with POACRT, and four were observed.

Administration of neoadjuvant pembrolizumab before surgery was safe. Serious immune-related AEs did not occur in the interval between administration of neoadjuvant pembrolizumab and through 30 days after surgery (**Table 2**). Unexpected surgical delays or complications were not observed (Supplementary Table S3). Delivery of POACRT was not compromised by prior neoadjuvant pembrolizumab. During administration of adjuvant pembrolizumab, one serious reversible immune-related AE occurred, hypothyroidism (**Table 2**).

Median follow-up after surgery was 22 months (interquartile range, 17.1–32.2); 97% had ≥1 year follow-up after surgery. In patients with high-risk pathology, the 1-year relapse rate was 16.7% (3/18, 95% CI, 3.6–41.4). In patients with low/intermediate-risk pathology, the 1-year relapse rate was 0% (Supplementary Figs. S1–S2).

After neoadjuvant pembrolizumab, pTR-2 occurred in the surgical specimens of eight patients (22%) and pTR-1 occurred in eight additional patients (22%). Overall, pTR of ≥10% was observed in 16 of 36 patients (44%; **Fig. 1B**; Supplementary Table S4). The proportion of patients who experienced pTR was similar in the high-risk and low/intermediate-risk pathology groups (**Fig. 1B**; Supplementary Table S5). Two patients had major pathologic response (>90%) in both the tumor and lymph nodes, but there were no pathologic complete responses. Of the patients with pTR and tumor in the primary site and lymph nodes, eight of 10 had pTR in only one of these sites.

Significant clinical tumor responses occurred in a minor proportion of patients after neoadjuvant pembrolizumab. Patient 20 experienced an exceptional clinical tumor response, and tumor downstaging (clinical stage IV: T_2N_{2b} downstaged to pathologic stage I: T_1N_0), after neoadjuvant pembrolizumab (**Fig. 1C–F**). The surgical specimen from this patient showed extensive pTR (90%), and only a small residual focus of SCC (**Fig. 1G**). Most patients had stable disease (**Fig. 1H**). The proportion of patients with high-risk pathology (50%) was lower than estimated (80%). Downstaging of cancer (defined as pathologic stage lower than clinical stage) after neoadjuvant pembrolizumab occurred in seven patients (19%; Supplementary Table S4).

We explored immunologic correlates of tumor response to neoadjuvant pembrolizumab using IHC, MIF, and RNA-seq performed on baseline and surgical samples. A positive correlation existed between PD-L1 protein expression in baseline biopsies and pTR (**Fig. 2A** and **B**, $r = 0.42$; 95% CI, 0.08–0.67; $P = 0.02$). MIF showed a positive correlation between extent of pTR and infiltration of $CD8^+$ ($r = 0.72$; 95% CI, 0.44–0.88; $P < 0.01$) but not $CD4^+$ T cells ($r = 0.27$; 95% CI: -0.16–0.62; $P = 0.20$) in baseline biopsies (**Fig. 2C** and **D**; Supplementary Fig. S3). These immune cell populations were queried by RNA-seq (26) and revealed significantly higher levels of overall immune infiltrate, M1 macrophages, and CD4 and CD8 T cells ($P < 0.05$) at baseline in patients with PTR compared with those without (**Fig. 3**; Supplementary Table S7). Consistent with these findings, differential gene expression analysis revealed that patients with PTR ($n = 6$) displayed significantly increased baseline expression of immune and inflammatory genes (e.g., *IFNG, CXCL9, CXCL10, CXCL11,* $P < 0.01$, FDR < 0.2) as well as significant enrichment of genes associated with these processes ($P < 0.01$, FDR < 0.2, **Fig. 3A**; Supplementary Table S8), compared with patients without PTR ($n = 10$). These inflammatory expression patterns were maintained in patients with PTR over treatment ($n = 4$).

Interestingly, comparing posttreatment, surgical samples from patients without PTR ($n = 11$) with matched baseline samples, posttreatment samples showed enrichment for inflammatory gene signatures ($P < 0.01$, FDR < 0.2) and increased expression of T-cell checkpoint molecules, including *PDCD1, CTLA4, ICOS, TIGIT, IDO1*,

Table 1. Patient characteristics by pathological risk category.

Characteristic	All patients ($N = 36$)	Patients with high-risk pathology ($N = 18$)	Patients with low/intermediate-risk pathology ($N = 18$)	*P* value[a]	Diff (95% CI)
Age at enrollment (years)					
Median (range)	60 (32–87)	61.5 (37–87)	58.5 (32–73)	0.16	5 (−2 to 13)
Sex, *N* (%)					
Male	26 (72)	13 (72)	13 (72)	1.00	0 (−29 to 29)
Female	10 (28)	5 (28)	5 (28)		
Ethnicity, *N* (%)					
White	28 (78)	15 (83)	13 (72)	0.82	11 (−16 to 38)
Black	6 (17)	2 (11)	4 (22)		−11 (−35 to 13)
Asian	2 (5)	1 (6)	1 (6)		0 (−15 to 15)
Smoking history, *N* (%)					
Ever	31 (86)	16 (89)	15 (83)	1.00	6 (−17 to 28)
Never	5 (14)	2 (11)	3 (17)		
Smoking pack-years					
Median (range)	30 (0–80)	30 (0–80)	30 (0–80)	0.79	0 (−15 to 10)
Alcohol use history, *N* (%)					
Ever	23 (64)	11 (61)	12 (67)	1.00	−6 (−37 to 26)
Never	13 (36)	7 (39)	6 (33)		
Eastern Cooperative Oncology Group performance status, *N* (%)					
0	26 (72)	16 (89)	10 (56)	0.06	33 (6 to 60)
1	10 (28)	2 (11)	8 (44)		
Tumor site, *N* (%)					
Larynx/hypopharynx	10 (28)	4 (22)	6 (33)	0.56	−11 (−4 to 18)
Oral cavity	22 (61)	11 (61)	11 (61)		0 (−32 to 32)
Oropharynx	4 (11)	3 (17)	1 (6)		11 (−9 to 31)
Clinical T stage, *N* (%)					
T1–T2	7 (19)	4 (22)	3 (17)	0.59	5 (−20 to 31)
T3	4 (11)	3 (17)	1 (6)		11 (−9 to 31)
T4	25 (69)	11 (61)	14 (78)		−17 (−46 to 31)
Clinical N stage, *N* (%)					
N0–N1	13 (36)	2 (11)	11 (61)	0.005	−50 (−77 to 23)
N2	21 (58)	14 (78)	7 (39)		39 (9 to 68)
N3	2 (6)	2 (11)	0		11 (−3 to 26)
Clinical disease stage, *N* (%)					
III	3 (8)	0	3 (17)	0.23	−17 (−34 to 1)
IV	33 (92)	18 (100)	15 (83)		
Days first visit to surgery					
Median (range)	33 (25–76)	35 (25–76)	33 (25–58)	0.81	1 (−5 to 11)
Days neoadjuvant pembrolizumab to surgery					
Median (range)	16 (13–22)	16 (13–22)	18 (14–22)	0.23	−1 (−3 to 1)
Pathologic disease stage, *N* (%)					
I–II	3 (8)	0	3 (17)	1.00	−17 (−34 to 1)
III	6 (17)	2 (11)	4 (22)		−11 (−35 to 13)
IVA–IVB	27 (75)	16 (89)	11 (61)		28 (10 to 55)

[a]Wilcoxon signed-rank test used for continuous variables; Fisher exact test used for categorical variables.

and *TNFSF4* ($P < 0.01$, FDR < 0.2, $n = 10$, **Fig. 3D**; Supplementary Fig. S4; Supplementary Table S8).

TCR sequencing was performed to assess the peripheral blood T-cell repertoire relationship to tumor-infiltrating immune-related expression patterns (22). We summarized the TCR repertoire using several metrics associated with either the clonality, richness, or diversity (see Supplementary Methods; ref. 27). There were no significant differences at baseline in the diversity, clonality, and richness in *TRB* clones of peripheral blood between patients without or with PTR. However, patients with PTR exhibited patterns associated with increased TCR diversity and clonality in peripheral blood after neoadjuvant pembrolizumab, with significantly higher Shannon, Gini Simpson, and Inverse Simpson diversity indices and lower geometric coefficient of variance ($P < 0.05$, Supplementary Figs. S5 and S6; ref. 27). Of note, there were 62 *TRA* (0–21 per patient) and 88 *TRB* (0–39 per patient) clonotypes that were also observed in bulk tumor RNA-seq data; these tumor-associated clones all ranked in the top 30.6% of clones detected in the peripheral blood (Supplementary Fig. S7).

We completed WES of DNA for 24 baseline and 22 surgical samples (25 patients, 21 matched pairs, average 91.3X coverage). Baseline tumor biopsies had nonsynonymous tumor mutation burden (TMB) ranging from 0.63 to 5.18 mutations/Mb (30–280 mutations), and the

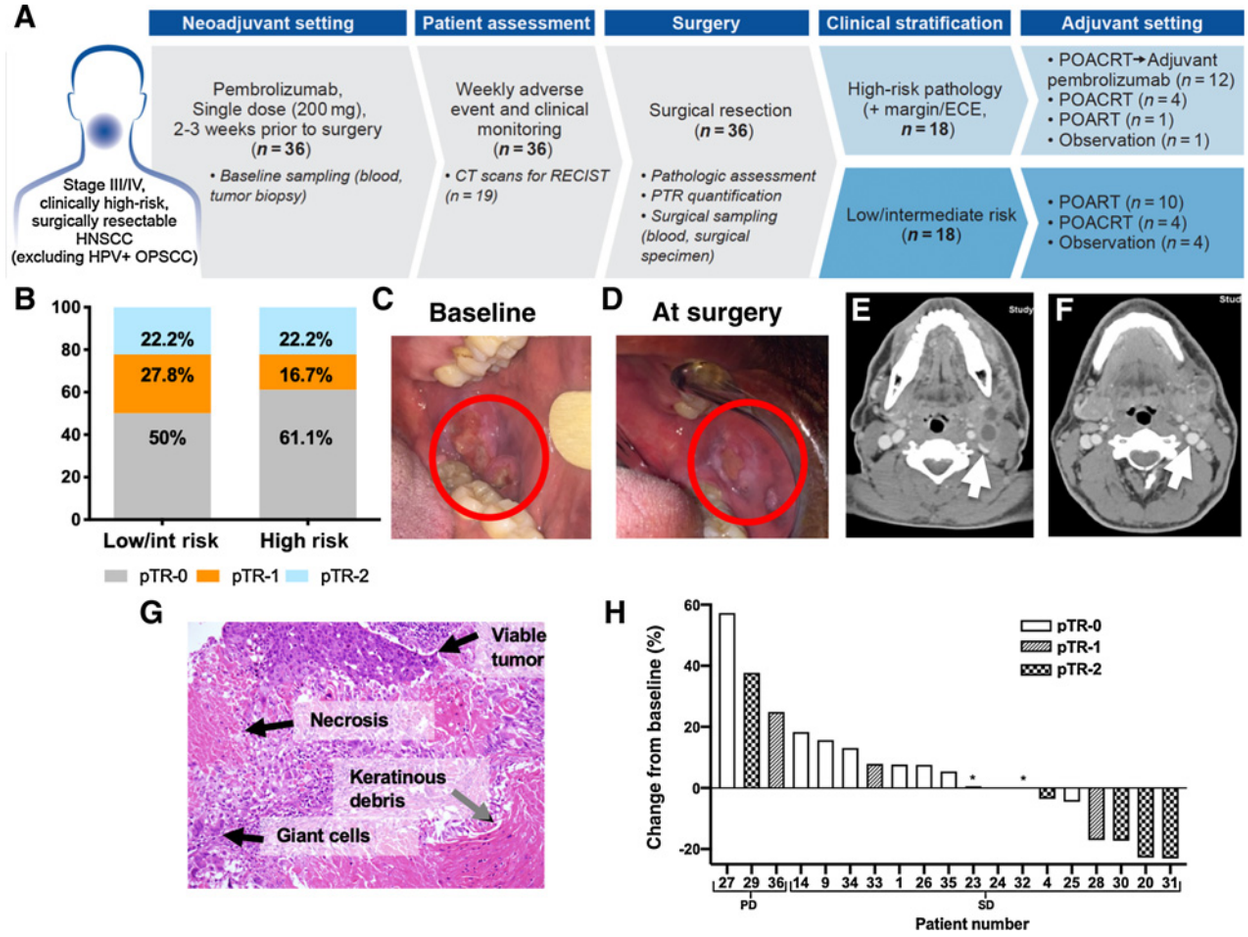

Figure 1.

Trial profile and tumor responses (pathologic and radiologic) to neoadjuvant pembrolizumab. **A,** Trial profile: Patients ($n = 36$) with locally advanced, stage III/IV, HPV-negative HNSCCs underwent baseline tumor and blood sampling and received neoadjuvant pembrolizumab 2 to 3 weeks before surgery. Of the 18 patients with high-risk pathology, 12 received adjuvant pembrolizumab. Patients with low/intermediate-risk pathology did not receive adjuvant pembrolizumab. **B,** Pathologic tumor response-2 (pTR-2) was observed in similar proportions of patients with low/intermediate- and high-risk pathology. Baseline (**C**) and postneoadjuvant (**D**) treatment (at surgery) images of oral cavity primary cancer in patient 20 showing dramatic decrease in the size. Representative CT images at (**E**) baseline and (**F**) after neoadjuvant pembrolizumab (day prior to surgery) confirmed tumor response seen on physical exam. Notably, the pretreatment CT and FDG-PET/CT scan (not shown) showed multiple large and necrotic FDG-avid neck lymph nodes, which are radiologic signs of SCC. Of note, the internal jugular vein (white arrow) was compressed on the baseline scan (**E**) and appeared fuller on the posttreatment scan (**F**). **G,** Representative hematoxylin and eosin slide of pTR highlighting changes noted in surgical specimens. **H,** Nineteen patients had CT evaluations at baseline and prior to surgery following neoadjuvant pembrolizumab: 16 with stable disease (SD) and three with progressive disease (PD) by RECIST criteria. *, Indicates two patients with pTR-1.

corresponding mutational landscape was consistent with that previously reported for HPV-unrelated HNSCC (Supplementary Fig. S8 and Supplementary Table S9; ref. 28). Neoantigens were predicted for each patient based upon their mutations (25) and inferred HLA haplotypes (29). Baseline, neoantigen burden ranged from 0 to 163 (median, 76) mutations. Baseline TMB and predicted neoantigen burden did not correlate with extent of PTR ($r = -0.27$, $P = 0.2$ and $r = -0.23$, $P = 0.29$, respectively; **Fig. 4**).

Comparing matched baseline and posttreatment tumor DNA, there were 2,431 variants (9–260 per patient, $n = 22$ patients with matched time points) that were detected in both baseline and posttreatment samples, and 873 variants (2–116 per patient) that were detected uniquely at a single time point (Supplementary Fig. S9) Variants detected solely at baseline could potentially indicate the event of immune rejection and clonal loss, whereas the emergence of variants posttreatment could indicate clonal expansion of a nonresponsive tumor clone or the presence of *de novo* tumor subclones. However, we hypothesized that some of these clonal dynamics may be observed due to insufficient sequencing depth or sampling bias. To address the impact of sequencing depth on the observed clonal dynamics, we designed a targeted capture probeset on WES-defined mutations (mean 160X coverage) to achieve higher sequencing depth (mean 1,060X coverage). Higher depth sequencing recovered 192 variants that were originally found at only one timepoint by WES, but there were still 615 variants (0–94 per patient) detected uniquely before or after treatment (Supplementary Fig. S9). Of note, clonal loss was not statistically significantly associated with pTR-1/2 ($P = 0.63$).

Alternatively, if the baseline and posttreatment surgical sections came from different regions of the tumor, spatial heterogeneity could also explain the presence of variants at either time point. Although

Table 2. Neoadjuvant and adjuvant pembrolizumab-related AEs.

	Neoadjuvant phase All patients ($N = 36$)		Postsurgery and adjuvant phase Patients treated with adjuvant pembrolizumab ($N = 12$)[a]	
Event	Grades 1–2 *N* (%)	Grades 3–4 *N* (%)	Grades 1–2 *N* (%)	Grades 3–4 *N* (%)
Fatigue	2 (6)	0 (0)	2 (17)	0 (0)
Hypothyroidism	0 (0)	0 (0)	3 (25)	1 (8)
Fever	1 (3)	0 (0)	0 (0)	0 (0)
Tumor flare	1 (3)	0 (0)	0 (0)	0 (0)
AST increase	0 (0)	0 (0)	1 (8)	0 (0)
ALT increase	0 (0)	0 (0)	1 (8)	0 (0)
Alk. phos. increase	0 (0)	0 (0)	1 (8)	0 (0)
Diarrhea	0 (0)	0 (0)	1 (8)	0 (0)

[a]No postsurgery/adjuvant phase pembrolizumab-related AEs occurred among patients who did not receive adjuvant pembrolizumab.

additional baseline samples were unavailable, we performed multisector analysis by microdissecting surgical resection samples. Formalin-fixed paraffin-embedded–preserved tumor sections from eight patients (41 samples, 3–8 per patient, Supplementary Fig. S10), obtained from geographically distinct regions in all remaining tumor blocks, were subjected to high-depth DNA sequencing using the custom capture probeset. Four patterns of tumor clonal dynamics were observed across the multisector analysis: (i) clonal conservation confirmed, (ii) clonal loss confirmed, (iii) clonal loss invalidated, and (iv) clonal expansion variable in some or all regions surveyed.

In some patients, mutations were conserved in baseline samples and across all posttreatment sections (e.g., patient 2, **Fig. 5**). To confirm clonal loss, variants identified as pretreatment-specific had to be completely absent in all regions of the posttreatment resected surgical specimen. There were 2–71 (median, 6.5) variants completely undetected in the original posttreatment specimens (denoted "PT1") across the eight patients with multisector sequencing, which was confirmed for 1–34 (median, 3) variants across all available matched posttreatment specimens. Clonal loss was especially evident in patients 15 (yellow cluster, Supplementary Fig. S11) and 16 (purple cluster, **Fig. 5**). On the other hand, there were 2–37 (median, 6) variants recovered in

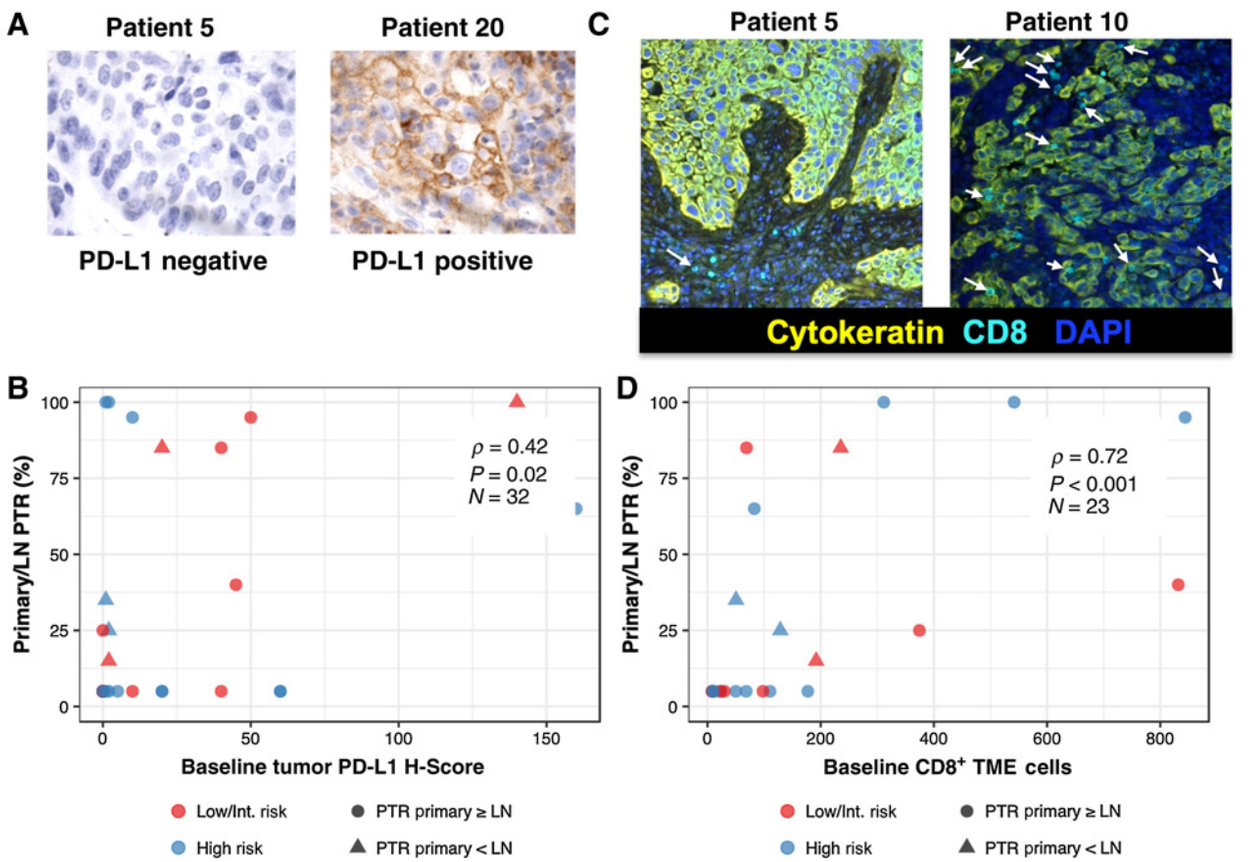

Figure 2.

PTR correlates with tumor PD-L1 and immune infiltrates. **A,** Representative PD-L1 staining of tumor biopsies at baseline. **B,** PD-L1 H-score correlated with PTR. Baseline PD-L1 primary tumor expression levels by IHC and percent PTR were significantly positively correlated for 32 evaluated patients (rho = 0.43; 95% CI, 0.079–0.668; **C**) representative MIF images showing patient 5 with minimal $CD8^+$ T-cell infiltrates and patient 10 with higher $CD8^+$ T-cell infiltrates (white arrows) in baseline biopsies. **D,** Extent of PTR was correlated with number of $CD8^+$ T cells in the baseline biopsy tumor microenvironment (TME). Baseline number of TME $CD8^+$ T cells assessed by MIF and percent PTR were significantly positively correlated for 23 evaluated patients (rho = 0.72; 95% CI, 0.443–0.875).

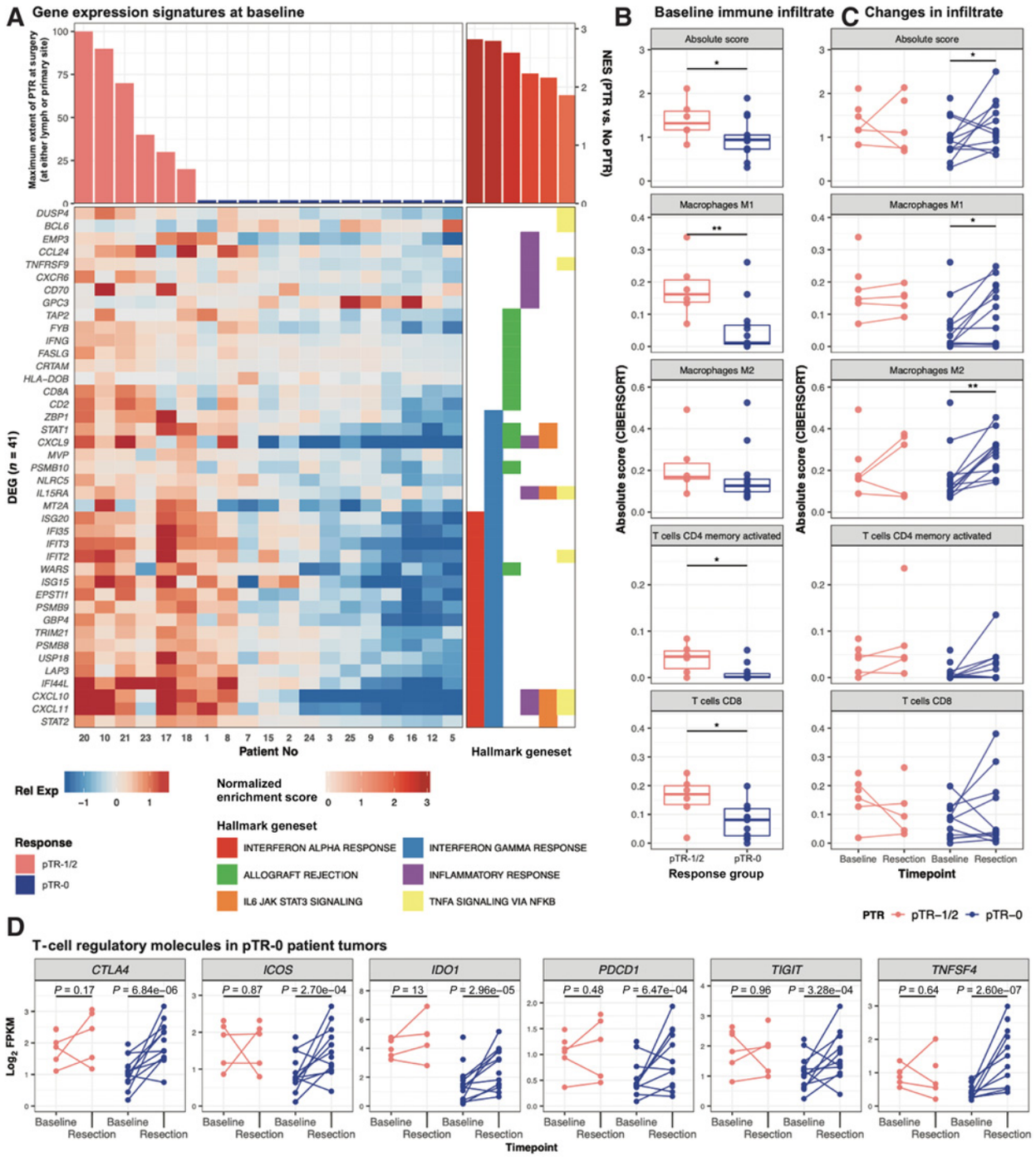

Figure 3.

Immune infiltrate and activity correspond to patient response. **A,** Heatmap shows genes ($n = 41$) associated with hallmark gene sets (right) that were differentially expressed ($P < 0.01$, adjusted $P < 0.25$) between patients with PTR and those without at baseline. Genes are sorted first by hallmark geneset, then by Ward's hierarchical clustering. Patients are sorted by decreasing maximum PTR (at either the tumor or lymph node site), then by Ward's hierarchical clustering. Expression is displayed as the gene-normalized expression across samples. **B** and **C,** Baseline- and posttreatment RNA was assessed for patterns of infiltrating immune cells, and values were summarized by the absolute levels of immune cells. These are indicated as the sum of all immune cell populations (absolute score) or by subpopulation at baseline (**B**). Matched samples were available for a subset of patients ($n = 15$), and the changes over the course of treatment are depicted by connected lines between baseline and resection time points in **C**. Wilcoxon tests were used to evaluate statistical significance across responder groups and time points; *, indicates $P < 0.05$. **D,** Expression (Log_2 FPKM, *y* axis) of six genes in baseline and posttreatment bulk tumor RNA-seq data. Points and lines are colored by either PTR (pTR-1/2) or without (pTR-0). Paired samples per individual are connected by lines, and *P* values (labeled above) indicate the comparison of paired pre- and posttreatment samples.

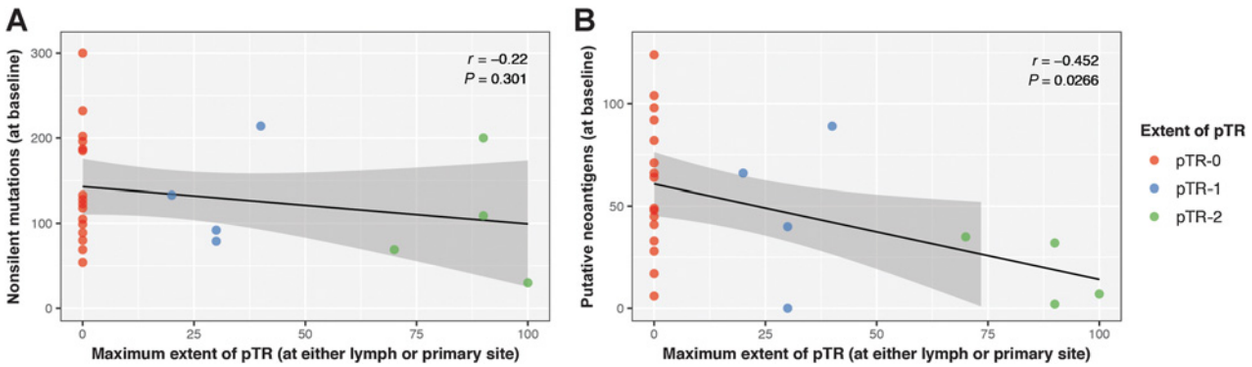

Figure 4.

Tumor mutational burden and neoantigen burden do not positively correlate with PTR. The number of (**A**) nonsilent mutations or (**B**) putative neoantigens predicted, as detected by WES and available RNA-seq data from baseline samples (*y* axes) was compared with the extent of PTR (*x* axis). "Extent of PTR" indicates the maximum PTR observed in the primary and/or resected lymph nodes. Points are colored by category of PTR, indicating whether there was no PTR (pTR-0), pTR-1 (<50% PTR at either site), or pTR-2 (>50% at either site).

at least one posttreatment sample, invalidating some original observations of clonal loss. For example, in patient 10 (pTR-2, orange and gold clusters, **Fig. 5**), an *NRAS* G13C activating mutation (42.4% baseline DNA VAF) was recovered in two of six additional samples (PT6-7).

In the original set of samples, there were 0–25 (median, 5.5) variants that were absent at baseline, suggesting the expansion of a novel or previously undetected subclone in seven patients. Clonal expansion patterns were validated across all posttreatment regions in patients 1 (pink cluster) and 15 (gold cluster, Supplementary Fig. S11), but there were 4–49 variants (median, 33) detected in only a subset of regions. These observations suggest that conclusions related to novel subclones or expansion are dependent upon spatial heterogeneity and sampling bias. For example, if PT3 or PT4 had originally been chosen for WES from patient 16, the clonal expansion observed in PT1 would not have been observed (see pink cluster, **Fig. 5**). Furthermore, because there was spatial heterogeneity posttreatment, there is strong evidence that this heterogeneity also existed at baseline. Therefore, we cannot discount the possibility that apparent clonal expansions might be invalidated if spatial heterogeneity at baseline could be assessed.

Discussion

To the best of our knowledge, we report the first application of an immune checkpoint inhibitor as a therapeutic strategy in patients with locally advanced, HPV-unrelated head and neck cancer. Administration of neoadjuvant pembrolizumab was safe and did not adversely affect the outcomes of surgery or the delivery of POACRT. Adjuvant pembrolizumab administered to patients with high-risk pathology was associated with a low risk of serious pembrolizumab-related AEs (8%).

In patients with locally advanced, HPV-unrelated HNSCC with high-risk pathology, we hypothesized that pembrolizumab administered before and after surgery would lower the rate of relapse. In our trial, the 1-year relapse rate in the 18 patients with high-risk pathology was 16.7%, lower than the historical rate of 35% (1, 2). These results should be cautiously interpreted because the sample size was small and the upper limit of the 95% CI for 1-year relapse rate included the historical relapse rate. An ongoing international phase III trial is testing the potential benefit of neoadjuvant and adjuvant pembrolizumab in patients with resectable, locally advanced HNSCC (NCT03765918).

In our trial, pTR-1 and pTR-2 occurred in 44% of patients after a single dose of neoadjuvant pembrolizumab. Patients with pTR ≥10% had better RFS compared with those without pTR. Although the sample size was small, these data provide the first evidence in patients with locally advanced HNSCC that pTR in response to neoadjuvant pembrolizumab may be a biomarker predictive of a lower rate of disease relapse. This hypothesis is being tested in an ongoing, phase III trial (NCT03765918). Pathologic complete response (pCR: absence of tumor in the surgical specimen) after one dose of neoadjuvant pembrolizumab did not occur. pCR rates of 15% to 45% were reported in other cancers (11–14); however, these trials administered multiple doses of one or combinations of immune checkpoint inhibitors. Discordant primary tumor and lymph node pTR were observed, but the biologic mechanism and clinical relevance of this finding are unclear.

We report the most comprehensive evaluation of tumor clonal loss following neoadjuvant immunotherapy, based upon high-depth and multisector genome sequencing of surgical specimens. Two prior studies suggested clonal loss after immunotherapy, but our study showed that depth of genome sequencing and spatial heterogeneity may influence the interpretation of clonal dynamics (30, 31). Clonal loss could be described in 19 cases using traditional WES approaches; five of these patients exhibited pTR. Targeted, high-depth sequencing recovered variants that were not detected by WES in posttreatment tumor DNA in three of 19 cases, invalidating these conclusions. However, with increased depth of sequencing, we still observed clonal loss in 16 cases (five with pTR). Using targeted genome sequencing of multiple sectors in a subset of cases, we were able to further validate clonal loss in two patients (patients 15 and 16; both pTR-0). In three cases [patients 5 (pTR-0), 10 (pTR-2), and 11 (pTR-0)], other sections showed persistence of clones that were originally considered "lost" by both WES and higher depth sequencing. Finding of tumor clonal loss by high-depth, multisector genome sequencing in some patients, including tumors with and without pTR, is further evidence of the antitumor effect of neoadjuvant pembrolizumab. However, we did not see a significant trend of clonal loss in patients with pTR. Thus, our findings strongly suggest that standard WES and calculated TMB from a single area, even if sampled from the same primary lesion before and after treatment, are not sufficient to make conclusions related to clonal dynamics due to insufficient sequencing depth and spatial heterogeneity. Furthermore, because we are often limited to a single, small biopsy from the lesion prior to treatment, these conclusions may be further influenced by spatial heterogeneity that was unevaluated at baseline.

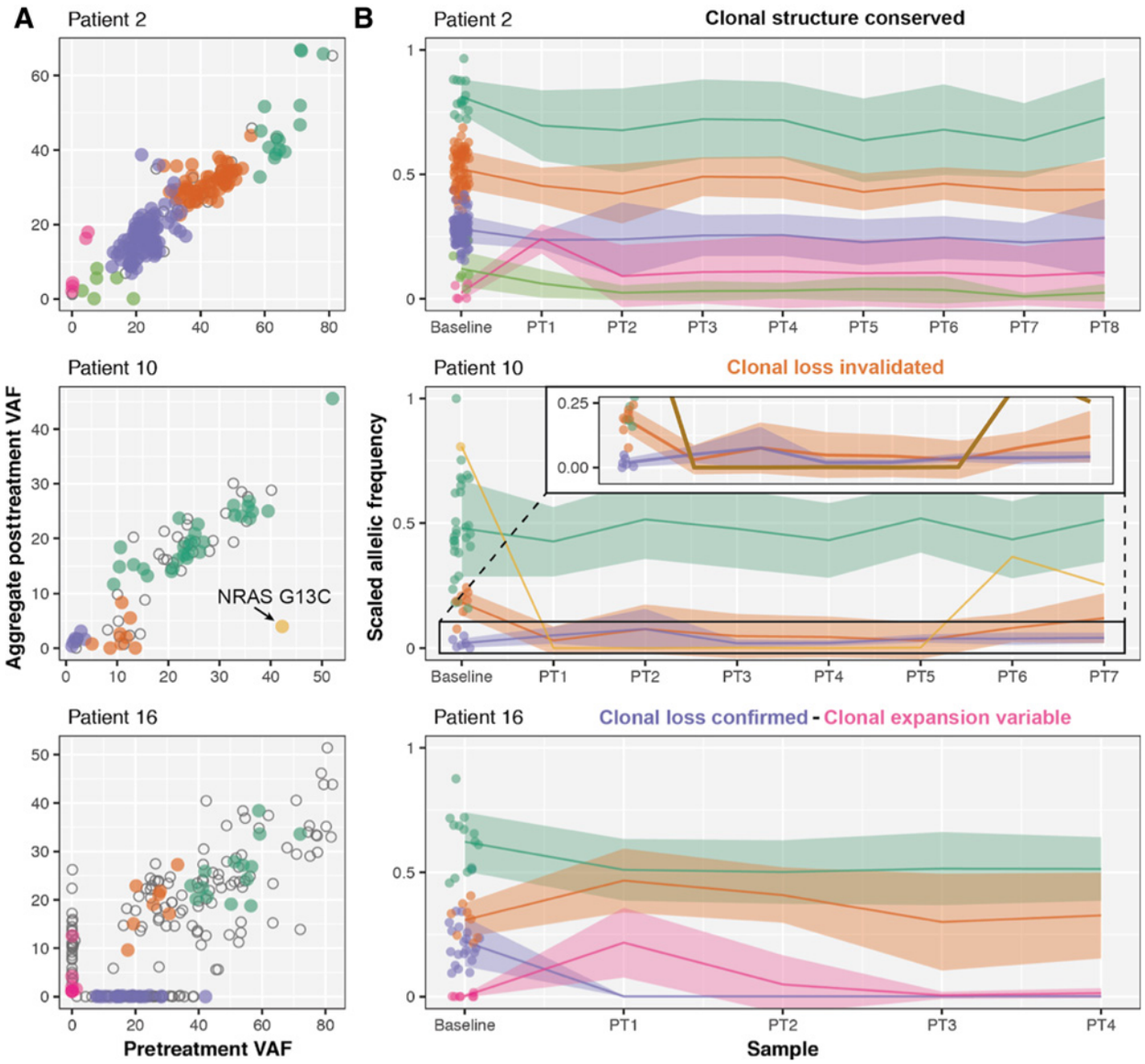

Figure 5.

Varied clonal dynamics due to spatial heterogeneity. **A,** Clonality plots comparing VAF of SNVs and Indels at baseline (*x* axis) and resection (*y* axis). These values represent aggregate metrics of all posttreatment samples available, and colors represent variants that clustered together by comparing these aggregate metrics per individual. Open circles represent variants that were either unassigned or were assigned to clusters with less than five variants. **B,** The scaled allelic frequency (AF) is depicted on the *y* axis of each variant (point) that was assigned a cluster in **A**. The solid line represents the average scaled AF of the cluster. Shaded ribbons represent the standard error from the mean scaled AF of the cluster. Eight nonoverlapping regions were isolated from patient 2 posttreatment (PT) resected tumor, seven regions were isolated from patient 10, and eight regions were isolated from patient 2 and analyzed (Supplementary Fig. S10).

Patients with pTR after neoadjuvant pembrolizumab had pre-existing primed immune effectors that were maintained over the course of treatment. pTR after neoadjuvant pembrolizumab correlated with baseline tumor PD-L1 expression, immune infiltrate, and IFNγ pathway activity, but not with TMB. The lack of association of TMB and tumor response in our cohort may be due to limited patient numbers. In other cancers, tumor response to anti–PD-1 therapy correlated with TMB and with metrics which described the baseline T-cell repertoire, infiltrating immune cell subpopulations, and expression patterns related to their activity (8, 32–35).

Our study provides insights into mechanisms of intrinsic resistance to anti–PD-1 therapy in patients with locally advanced HNSCC. Patients who did not experience pTR after neoadjuvant pembrolizumab showed limited immune activity in the baseline tumor specimen. A subset of these patients showed upregulation of immune pathways in the surgical sample after neoadjuvant pembrolizumab; however, this was counterbalanced by increased expression of T-cell checkpoint molecules, including *PDCD1, CTLA4, ICOS, TIGIT, IDO1*, and *TNFSF4*. These observations show that one dose of neoadjuvant pembrolizumab promoted enhanced

inflammatory gene signatures in some patients without pTR, and raise the possibility that additional doses of neoadjuvant pembrolizumab, or addition of therapy targeting different immune checkpoints, could increase the proportion of patients with pTR. In preclinical models, targeting immune checkpoint inhibitor compensatory responses enabled bypass of single immune checkpoint inhibitor resistance (36, 37). Importantly, it is also possible that a single dose of pembrolizumab induces an adaptive immune suppression. Note that 24 of 36 patients received only one dose of neoadjuvant pembrolizumab, and 12 of 36 received neoadjuvant and adjuvant cycles. In melanoma, a single dose of neoadjuvant pembrolizumab in patients with stage IIIB/C or IV melanoma was predictive of clinical outcomes (17). Whether adaptive immune suppression is induced by neoadjuvant dosing or whether a single dose is predictive of clinical outcomes in HNSCC should be addressed in future trials defining the testing different numbers of doses in the neoadjuvant period.

After neoadjuvant pembrolizumab, we observed tumor downstaging in 19% of patients. Also, the rate of high-risk pathology (50%) was slightly lower than historical (68%). These outcomes were unexpected and must be confirmed in prospective controlled trials. The importance of these observations is that they could alter recommendations for adjuvant therapy. The best example of the potential to alter adjuvant therapy recommendations was patient 20, who presented with clinical stage IV (T2N2bM0) buccal SCC. After neoadjuvant pembrolizumab, the surgery specimen showed pathologic stage I (T1N0) disease. Extensive pTR was present, and only a 5-mm residual focus of carcinoma. In the absence of adjuvant therapy, the patient remained free of disease 29 months after surgery. Neoadjuvant immunotherapy has the potential to reduce the intensity of adjuvant therapy in patients with resectable, locally advanced HNSCC. However, our trial is limited in size as described below, and this hypothesis needs rigorous validation in ongoing trials that evaluate and test the safety and/or efficacy of modifying standard-of-care adjuvant treatment paradigms when incorporating immunotherapy.

Our trial has several limitations. The patient sample size was small, and the study design did not include a placebo-controlled arm. The proportion of patients with high-risk pathology was lower than expected, which resulted in fewer patients given adjuvant pembrolizumab. The standard-of-care adjuvant therapy varied. We cannot conclude the safety or benefit of adjuvant pembrolizumab given the limited sample size. Due to the limited size of pretreatment biopsies, we were unable to perform multisector, targeted genome sequencing in baseline tumor samples. Several biomarkers correlated with achievement of PTR to neoadjuvant pembrolizumab, but we were unable to address which biomarker was best suited to predict pTR. Relapse events through 1-year after surgery were mature; however, longer follow-up is needed, because immunotherapy could delay the appearance of relapse events.

In conclusion, neoadjuvant pembrolizumab administered to patients with resectable locally advanced, HPV-unrelated HNSCC was safe and resulted in pTR in 44% of patients and a 1-year relapse rate lower than historical in patients with high-risk pathology. High-depth, multisector genome sequencing of surgical specimens documented tumor clonal loss after neoadjuvant pembrolizumab and highlighted the importance of accounting for spatial heterogeneity. Correlates of pTR with biomarkers of response and potential mechanisms of resistance to pembrolizumab were shown. Further studies of neoadjuvant pembrolizumab in patients with resectable locally advanced, HPV-unrelated HNSCC are warranted.

Disclosure of Potential Conflicts of Interest

R. Uppaluri reports grants and personal fees from Merck Inc. K.M. Campbell reports being a shareholder in Geneoscopy LLC. P. Oppelt reports personal fees from Merck, Bristol Myers Squibb, and Eisai outside the submitted work. G.P. Dunn reports other from Immunovalent (Co-founder) outside the submitted work. E.K. Barnell reports other from Geneoscopy (stock, equity, and board member) outside the submitted work, and is listed as a co-inventor on a provisional patent application on methods for isolating eukaryotic RNA from stool that is owned by Geneoscopy Inc. T.J. Pugh is listed as a co-inventor on a provisional patent application on immune repertoire capture and sequencing that is owned by University Health Network. G.J. Hanna reports personal fees and non-financial support from BMS, Exicure, Kite Pharma, Regeneron, and Sanofi Genzyme, grants from ASCO/CCF and Gateway for Cancer Research, and personal fees from Merck and Bicara outside the submitted work. R. Haddad reports personal fees from BMS, MERCK, AZ, GSK, PFIZER, GENENTECH, IO BIOTECH, KURA, and EISAI during the conduct of the study; other from BMS, Merck, Pfizer, Kura, AstraZeneca, Genentech, and GSK (Research Support) outside the submitted work. J.D. Schoenfeld reports other from Merck (paid to the institution) during the conduct of the study; grants from Regeneron and Merck, personal fees from Debiopharm Group, ACI, Immunitas (SAB, equity), pKline & Spector PC, Heidell, Pittoni, Murphy and Bach, Catenion, LEK, TILOS, AstraZeneca, and Nanobiotix, and grants and personal fees from BMS outside the submitted work. A. Lako reports other from Bristol Myers Squibb (Employment) outside the submitted work. S.J. Rodig reports grants from Bristol Myers Squibb (Research support unrelated to this project), Merck (Research support unrelated to this project), Affimed (Research support unrelated to this project), and gKITE/Gilead (Research support unrelated to this project) outside the submitted work; is on a scientific advisory board for Immunitas, and received limited stock in the company, and is on a scientific advisory board for Rarecyte which is unrelated to this project. I.S. Hagemann reports personal fees from Change Healthcare outside the submitted work. D. Kallogjeri is a statistics editor for JAMA Otolaryngology Head and neck surgery, owns stock and served as consultant for PotentiaMetrics. R.D. Chernock reports personal fees from Roche (Advisory Board Member) and Merck (Consultant) during the conduct of the study. O.L. Griffith reports grants from V Foundation, NIH, and Cancer Research Foundation during the conduct of the study. D.R. Adkins reports grants and personal fees from Merck (research funding and advisory board) during the conduct of the study; Pfizer (research funding and advisory board), Eli Lilly (research funding and advisory board), Celgene - now BMS (research funding and advisory board), Cue Biopharma (research funding and advisory board), personal fees from Loxo Oncology (advisory board), grants from Novartis (research funding), Roche (research funding), Aduro (research funding), Atara (research funding), Matrix (research funding), Blueprint Medicine (research funding), Celldex (research funding), Enzychem (research funding), Exilixis (research funding), Shanghai De Novo (research funding), Kura (research funding), Astrazeneca (research funding), Medimmune (research funding), and Innate (research funding) outside the submitted work. No potential conflicts of interest were disclosed by the other authors.

Authors' Contributions

R. Uppaluri: Conceptualization, resources, data curation, formal analysis, supervision, funding acquisition, investigation, visualization, methodology, writing-original draft, project administration, writing-review and editing. **K.M. Campbell:** Conceptualization, data curation, software, formal analysis, validation, investigation, visualization, methodology, writing-original draft, writing-review and editing. **A.M. Egloff:** Data curation, formal analysis, validation, investigation, writing-review and editing. **P. Zolkind:** Investigation, writing-review and editing. **Z.L. Skidmore:** Data curation, software, formal analysis, investigation, visualization, writing-review and editing. **B. Nussenbaum:** Resources, writing-review and editing. **R.C. Paniello:** Resources, writing-review and editing. **J.T. Rich:** Resources, writing-review and editing. **R. Jackson:** Resources, writing-review and editing. **P. Pipkorn:** Resources, writing-review and editing. **L.S. Michel:** Resources, writing-review and editing. **J. Ley:** Data curation, supervision, writing-review and editing. **P. Oppelt:** Resources, writing-review and editing. **G.P. Dunn:** Resources, investigation, writing-review and editing. **E.K. Barnell:** Data curation, software, formal analysis, visualization, writing-review and editing. **N.C. Spies:** Software, formal analysis, visualization, writing-review and editing. **T. Lin:** Investigation. **T. Li:** Investigation. **D.T. Mulder:** Investigation. **Y. Hanna:** Investigation. **I. Cirlan:** Investigation. **T.J. Pugh:** Investigation, methodology, writing-review and editing. **T. Mudianto:** Investigation. **R. Riley:** Investigation. **L. Zhou:** Investigation. **V.Y. Jo:** Investigation, writing-review and editing. **M.D. Stachler:** Investigation. **G.J. Hanna:** Resources, writing-review and editing. **J. Kass:** Resources. **R. Haddad:** Resources, writing-review and editing. **J.D. Schoenfeld:** Resources, investigation, writing-review and editing. **E. Gjini:** Investigation, visualization.

A. Lako: Investigation, visualization. **W. Thorstad:** Resources, investigation, writing-review and editing. **H.A. Gay:** Resources. **M. Daly:** Resources. **S.J. Rodig:** Formal analysis, supervision, methodology, writing-review and editing. **I.S. Hagemann:** Validation, investigation. **D. Kallogjeri:** Data curation, software, formal analysis, investigation, methodology, writing-review and editing. **J.F. Piccirillo:** Data curation, formal analysis, supervision, investigation, methodology, writing-review and editing. **R.D. Chernock:** Conceptualization, validation, investigation, visualization, writing-review and editing. **M. Griffith:** Data curation, software, formal analysis, supervision, investigation, visualization, methodology, writing-review and editing. **O.L. Griffith:** Conceptualization, data curation, software, formal analysis, supervision, funding acquisition, validation, investigation, visualization, methodology, writing-original draft, project administration. **D.R. Adkins:** Conceptualization, resources, formal analysis, supervision, funding acquisition, investigation, methodology, writing-original draft, project administration.

Acknowledgments

We thank all patients and their families for their participation in this study. We recognize the support of the Alvin J. Siteman Cancer Center at Washington University School of Medicine and Barnes-Jewish Hospital in St. Louis, Missouri, the Clinical Trials Core, the Biostatistics Shared Resource, and the Center for Biomedical Informatics. The Siteman Cancer Center is supported in part by NCI Cancer Center Support Grant #P30 CA91842. M. Griffith is funded by the National Human Genome Research Institute (NIH NHGRI R00HG007940), O.L. Griffith by the National Cancer Institute (NIH/NCI K22CA188163, NIH/NCI U01CA209936, and NIH/NCI U24CA237719), and a Cancer Research Foundation Young Investigator Award. R. Uppaluri is funded by the National Institute for Dental and Craniofacial Research (NIH/NIDCR R01DE024403, R01DE027736) and a V Foundation Translational Research Award. Clinical trial support was through a Merck Investigator Studies Program award to R. Uppaluri/D.R. Adkins.

The costs of publication of this article were defrayed in part by the payment of page charges. This article must therefore be hereby marked *advertisement* in accordance with 18 U.S.C. Section 1734 solely to indicate this fact.

Received May 3, 2020; revised June 8, 2020; accepted July 8, 2020; published first July 14, 2020.

References

1. Cooper JS, Pajak TF, Forastiere AA, Jacobs J, Campbell BH, Saxman SB, et al. Postoperative concurrent radiotherapy and chemotherapy for high-risk squamous-cell carcinoma of the head and neck. N Engl J Med 2004;350:1937–44.
2. Bernier J, Domenge C, Ozsahin M, Matuszewska K, Lefèbvre J-L, Greiner RH, et al. Postoperative irradiation with or without concomitant chemotherapy for locally advanced head and neck cancer. N Engl J Med 2004;350:1945–52.
3. Harrington K, Temam S, Mehanna H, D'Cruz A, Jain M, D'Onofrio I, et al. Postoperative adjuvant lapatinib and concurrent chemoradiotherapy followed by maintenance lapatinib monotherapy in high-risk patients with resected squamous cell carcinoma of the head and neck: a phase III, randomized, double-blind, placebo-controlled study. J Clin Oncol 2015;33:4202–9.
4. Ferris RL, Blumenschein G, Fayette J, Guigay J, Colevas AD, Licitra L, et al. Nivolumab for recurrent squamous-cell carcinoma of the head and neck. N Engl J Med 2016;375:1856–67.
5. Cohen EEW, Soulières D, Le Tourneau C, Dinis J, Licitra L, Ahn M-J, et al. Pembrolizumab versus methotrexate, docetaxel, or cetuximab for recurrent or metastatic head-and-neck squamous cell carcinoma (KEYNOTE-040): a randomised, open-label, phase 3 study. Lancet 2019;393:156–67.
6. Burtness B, Harrington KJ, Greil R, Soulières D, Tahara M, De Castro G, et al. LBA8_PRKEYNOTE-048: phase III study of first-line pembrolizumab (P) for recurrent/metastatic head and neck squamous cell carcinoma (R/M HNSCC). Lancet 2019;23:394(10212):1915–28. doi: 10.1016/S0140-6736(19)32591-7.
7. Liu J, Blake SJ, Yong MCR, Harjunpää H, Ngiow SF, Takeda K, et al. Improved efficacy of neoadjuvant compared to adjuvant immunotherapy to eradicate metastatic disease. Cancer Discov 2016;6:1382–99.
8. Liu J, O'Donnell JS, Yan J, Madore J, Allen S, Smyth MJ, et al. Timing of neoadjuvant immunotherapy in relation to surgery is crucial for outcome. Oncoimmunology 2019;8:e1581530.
9. Friedman J, Moore EC, Zolkind P, Robbins Y, Clavijo PE, Sun L, et al. Neoadjuvant PD-1 immune checkpoint blockade reverses functional immunodominance among tumor antigen-specific T cells. Clin Cancer Res 2020;26:679–89.
10. Hanna GJ, Adkins DR, Zolkind P, Uppaluri R. Rationale for neoadjuvant immunotherapy in head and neck squamous cell carcinoma. Oral Oncol 2017;73:65–9.
11. Forde PM, Chaft JE, Smith KN, Anagnostou V, Cottrell TR, Hellmann MD, et al. Neoadjuvant PD-1 blockade in resectable lung cancer. N Engl J Med 2018;378:1976–86.
12. Amaria RN, Reddy SM, Tawbi HA, Davies MA, Ross MI, Glitza IC, et al. Neoadjuvant immune checkpoint blockade in high-risk resectable melanoma. Nat Med 2018;24:1649–54.
13. Blank CU, Rozeman EA, Fanchi LF, Sikorska K, van de Wiel B, Kvistborg P, et al. Neoadjuvant versus adjuvant ipilimumab plus nivolumab in macroscopic stage III melanoma. Nat Med 2018;24:1655–61.
14. Necchi A, Anichini A, Raggi D, Briganti A, Massa S, Lucianò R, et al. Pembrolizumab as neoadjuvant therapy before radical cystectomy in patients with muscle-invasive urothelial bladder carcinoma (PURE-01): an open-label, single-arm, phase II study. J Clin Oncol 2018;36:3353–60.
15. Cloughesy TF, Mochizuki AY, Orpilla JR, Hugo W, Lee AH, Davidson TB, et al. Neoadjuvant anti-PD-1 immunotherapy promotes a survival benefit with intratumoral and systemic immune responses in recurrent glioblastoma. Nat Med 2019;25:477–86
16. Schalper KA, Rodriguez-Ruiz ME, Diez-Valle R, López-Janeiro A, Porciuncula A, Idoate MA, et al. Neoadjuvant nivolumab modifies the tumor immune microenvironment in resectable glioblastoma. Nat Med 2019;25:470–6.
17. Huang AC, Orlowski RJ, Xu X, Mick R, George SM, Yan PK, et al. A single dose of neoadjuvant PD-1 blockade predicts clinical outcomes in resectable melanoma. Nat Med 2019;25:454–61.
18. Ferrarotto R, Bell D, Rubin ML, Hutcheson KA, Johnson JM, Goepfert RP, et al. Impact of neoadjuvant durvalumab with or without tremelimumab on CD8+ tumor lymphocyte density, safety, and efficacy in patients with oropharynx cancer: CIAO trial. Clin Cancer Res 2020;26:3211–9.
19. Topalian SL, Bhatia S, Amin A, Kudchadkar RR, Sharfman WH, Lebbé C, et al. Neoadjuvant nivolumab for patients with resectable merkel cell carcinoma in the checkmate 358 trial. J Clin Oncol 2020;JCO2000201.
20. Chalabi M, Fanchi LF, Dijkstra KK, Van den Berg JG, Aalbers AG, Sikorska K, et al. Neoadjuvant immunotherapy leads to pathological responses in MMR-proficient and MMR-deficient early-stage colon cancers. Nat Med 2020;26:566–76.
21. Dindo D, Demartines N, Clavien P-A. Classification of surgical complications: a new proposal with evaluation in a cohort of 6336 patients and results of a survey. Ann Surg 2004;240:205–13.
22. Mulder DT, Mahé ER, Dowar M, Hanna Y, Li T, Nguyen LT, et al. CapTCR-seq: hybrid capture for T-cell receptor repertoire profiling. Blood Adv 2018;2:3506–14.
23. Griffith M, Griffith OL, Smith SM, Ramu A, Callaway MB, Brummett AM, et al. Genome modeling system: a knowledge management platform for genomics. PLoS Comput Biol 2015;11:e1004274.
24. Campbell KM, Lin T, Zolkind P, Barnell EK, Skidmore ZL, Winkler AE, et al. Oral cavity squamous cell carcinoma xenografts retain complex genotypes and intertumor molecular heterogeneity. Cell Rep 2018;24:2167–78.
25. Hundal J, Carreno BM, Petti AA, Linette GP, Griffith OL, Mardis ER, et al. pVAC-Seq: A genome-guided in silico approach to identifying tumor neoantigens. Genome Med 2016;8:11.
26. Newman AM, Liu CL, Green MR, Gentles AJ, Feng W, Xu Y, et al. Robust enumeration of cell subsets from tissue expression profiles. Nat Methods 2015;12:453–7.
27. Zhang L, Cham J, Paciorek A, Trager J, Sheikh N, Fong L. 3D: diversity, dynamics, differential testing - a proposed pipeline for analysis of next-generation sequencing T cell repertoire data. BMC Bioinformatics 2017;18:129.
28. Cancer Genome Atlas Network. Comprehensive genomic characterization of head and neck squamous cell carcinomas. Nature 2015;517:576–82.
29. Xie C, Yeo ZX, Wong M, Piper J, Long T, Kirkness EF, et al. Fast and accurate HLA typing from short-read next-generation sequence data with xHLA. Proc Natl Acad Sci U S A 2017;114:8059–64.
30. Riaz N, Havel JJ, Makarov V, Desrichard A, Urba WJ, Sims JS, et al. Tumor and microenvironment evolution during immunotherapy with nivolumab. Cell 2017;171:934–49.e15.

31. Anagnostou V, Smith KN, Forde PM, Niknafs N, Bhattacharya R, White J, et al. Evolution of neoantigen landscape during immune checkpoint blockade in non-small cell lung cancer. Cancer Discov 2017;7:264–76.
32. Funt SA, Chapman PB. The role of neoadjuvant trials in drug development for solid tumors. Clin Cancer Res 2016;22:2323–8.
33. Martin ST, Heneghan HM, Winter DC. Systematic review and meta-analysis of outcomes following pathological complete response to neoadjuvant chemoradiotherapy for rectal cancer. Br J Surg 2012;99:918–28.
34. Cottrell TR, Thompson ED, Forde PM, Stein JE, Duffield AS, Anagnostou V, et al. Pathologic features of response to neoadjuvant anti-PD-1 in resected non-small-cell lung carcinoma: a proposal for quantitative immune-related pathologic response criteria (irPRC). Ann Oncol 2018;29:1853–60.
35. Tetzlaff MT, Messina JL, Stein JE, Xu X, Amaria RN, Blank CU, et al. Pathological assessment of resection specimens after neoadjuvant therapy for metastatic melanoma. Ann Oncol 2018;29:1861–8.
36. Huang R-Y, Francois A, McGray AR, Miliotto A, Odunsi K. Compensatory upregulation of PD-1, LAG-3, and CTLA-4 limits the efficacy of single-agent checkpoint blockade in metastatic ovarian cancer. Oncoimmunology 2017;6:e1249561.
37. Koyama S, Akbay EA, Li YY, Herter-Sprie GS, Buczkowski KA, Richards WG, et al. Adaptive resistance to therapeutic PD-1 blockade is associated with upregulation of alternative immune checkpoints. Nat Commun 2016;7:10501.